

Enhanced index of refraction in four-wave mixing media

Elena Kuznetsova,^{1,2,3} Renuka Rajapakse,¹ and S. F. Yelin^{1,2,4}

¹*Department of Physics, University of Connecticut, Storrs, CT 06269*

²*ITAMP, Harvard-Smithsonian Center for Astrophysics, Cambridge, MA 02138*

³*Russian Quantum Center, 100 Novaya Street, Skolkovo, Moscow region, 143025, Russia*

⁴*Department of Physics, Harvard University, Cambridge, MA 02138*

(Dated: August 7, 2018)

Refractive index enhancement accompanied by vanishing absorption in a four-level atomic system interacting with two control and two probe fields in a regime of four-wave mixing (FWM) has been predicted and studied in the present work. We analyzed the maximal index enhancement in the four-level FWM system and gave index estimates for a real atomic gas of ^{40}K , taking into account its multilevel structure and collisional and Doppler broadenings at large atomic densities. We also discussed how vanishing absorption with no nearby amplification can be realized in a two species system, consisting of a four-level FWM and a two-level system, where the latter provides additional absorption for one of the probe fields. We numerically estimated the index change in a system composed of ^{40}K and ^{39}K gases.

PACS numbers:

I. INTRODUCTION

Refractive index governs light propagation in macroscopic materials, resulting in everyday phenomena such as light refraction, reflection and absorption [1]. For a long time the index of refraction was considered given by nature and could be changed only by choosing an appropriate material. In recent decades this situation has changed in two different ways: 1) control of material optical response using external fields and 2) artificial materials (metamaterials) have been realized. One of the best examples of the first kind is electromagnetically induced transparency (EIT), which reduces absorption of a resonant probe field by irradiating a medium with a strong control field thus making an otherwise opaque medium transparent [2]. It also changes dramatically the group velocity of light, reducing it down to cm/s or even stopping a light pulse completely by converting it into a material excitation [3, 4]. Control of the group velocity is important for many applications such as optical delay lines and memories, but the refractive index itself is also of great interest. For example, negative index of refraction, proposed by Veselago [5], can provide imaging with unlimited resolution allowing one to build a perfect lens [6]. On the opposite side, enhanced refractive index attracts significant attention as well. It is well known that spatial resolution of optical imaging techniques is given by the focus size of a light wave, which is diffraction limited to λ^2 . Overcoming this limit and reducing the minimal image feature size is one of the main goals in spectroscopy nowadays [7]. Enhanced refractive index leads to a decreased wavelength of an electromagnetic wave in a medium $\lambda = \omega/cn$, where n is the real part of the complex refractive index. Thus light with shorter wavelengths in high index media can find applications in lithography and optical imaging. Another exciting application of enhanced refractive index is invisibility cloaking, allowing to hide an object from light by tailoring the

material index around it [8].

Refractive index can be controlled using external fields in analogy to group velocity. It is well known that in a medium composed of two-level atoms the index of refraction for a near resonant light can be high, but absorption, given by the imaginary part of the complex index, is of the same order. It results in light attenuation by $1/e$ at a distance corresponding to the accumulated phase ~ 1 rad, making this approach impractical. In order to eliminate absorption and have at the same time enhanced index of refraction two schemes have been suggested for laser controlled atomic media. The first one pioneered by Scully [11] utilizes a long-lived coherence at a low-frequency transition in a three-level Λ -type atomic system. The coherence modifies the medium susceptibility and allows one to cancel probe absorption at some frequency, having at the same time non-vanishing refractive index. The second approach, proposed by Yavuz [13], does not require atomic coherence and uses a superposition of two-level absorbing and amplifying resonances, shown in Fig.1a. There is a frequency corresponding to vanishing absorption between the resonances accompanied by non-zero refractive index. The main difficulty of both approaches is that there is an amplification region next to the zero absorption point and if the field frequency fluctuates around this point the fluctuations get amplified. To overcome this problem it was proposed in [14] to use two overlapping resonances of different width: a wide absorbing and a narrow amplifying one. In this case vanishing absorption with no nearby amplification can be realized (see Fig.1d).

The remaining difficulty of the absorbing/amplifying system of [13, 14] is the need for either direct or Raman inversion at the amplifying transition. Direct inversion in two-level systems is difficult to realize and maintain. Raman inversion in three-level species is easier to maintain but requires first pumping population in one of the two ground states. In the scheme used in [15] where absorb-

ing and amplifying resonances were realized with ^{87}Rb and ^{85}Rb gases, cross-coupling between optical pumping processes in the two species limited index enhancement to $\Delta n \approx 2 \times 10^{-7}$. In a more optimal case of [16] where the absorbing and amplifying transitions were realized in a single atomic species, population had to be optically pumped into a single ground state sublevel. In this case optical pumping worked well for atomic densities $N < 1.2 \cdot 10^{14} \text{ cm}^{-3}$, also limiting index enhancement to $\Delta n \sim 10^{-4}$. The index change obtained using the atomic coherence based approach of Scully [12] was also limited to $\Delta n \sim 10^{-4}$ due to population pumping into dark hyperfine states reducing the number of atoms actively interacting with light.

We propose a more robust scheme for realization of enhanced refractive index based on a four-wave mixing (FWM) system, shown in Fig.2a. In our approach an atomic coherence provides the enhanced index combined with vanishing absorption similar to [11]. The FWM scheme, however, can be realized without any kind of optical pumping, inversion or population transfer in dark states making it easier and more robust compared to both the coherence based and the absorbing/amplifying systems.

The paper is organized as follows. In Section IIa we remind the index enhancement approach based on two-level atomic species providing absorbing and amplifying resonances for a probe field. In Section IIb we analyze the complex refractive index for a medium composed of four-level atoms in the regime of four-wave mixing. In Section IIc we consider the possibility to realize index enhancement with vanishing absorption and no amplification regions nearby. Finally, we conclude in Section III.

II. INDEX ENHANCEMENT IN AN ABSORBING/AMPLIFYING MEDIUM

In the approach of [13, 14] a two-component atomic medium is used, in which one species provides absorption for a probe field while the other species provides amplification. Absorption and amplification can be realized either with two-level (see Fig.1a) or three-level Raman systems. In practice it is difficult to realize and maintain inversion at optical transitions, and therefore Raman transitions are used. The equivalent of Fig.1a for Raman transitions is shown in Fig.1b, which uses two Raman systems with all population in the ground states $|g\rangle$, $|g'\rangle$, driven by two strong control fields E_{c1} , E_{c2} and interacting with the same weak probe field E_p . The probe and the control fields are near two-photon resonant with low frequency transitions $|g\rangle - |1\rangle$, $|g'\rangle - |1'\rangle$ and the probe field is absorbed at the $|g\rangle - |e\rangle$ and amplified at the $|e'\rangle - |1'\rangle$ transitions. This scheme can be realized using either two atomic species as in Fig.1b or different transitions in the same atomic species as was done in the experiment [16]. The change of the refractive index

induced by the absorbing/amplifying system of Fig.1a, which we consider for simplicity, is given by

$$\Delta n = \frac{2\pi i}{\hbar} \left(\frac{N|\mu_{21}|^2(\rho_{11} - \rho_{22})}{i\Delta + \gamma} + \frac{N'|\mu_{2'1'}|^2(\rho'_{11} - \rho'_{22})}{i\Delta' + \gamma'} \right), \quad (1)$$

where N , N' are atomic densities of the first and second species, μ_{21} , $\mu_{2'1'}$ are the dipole moments of the corresponding transitions, Δ , Δ' are the detunings of the probe field from the $|2\rangle - |1\rangle$ and $|2'\rangle - |1'\rangle$ transitions, and γ and γ' are the optical coherence decay rates.

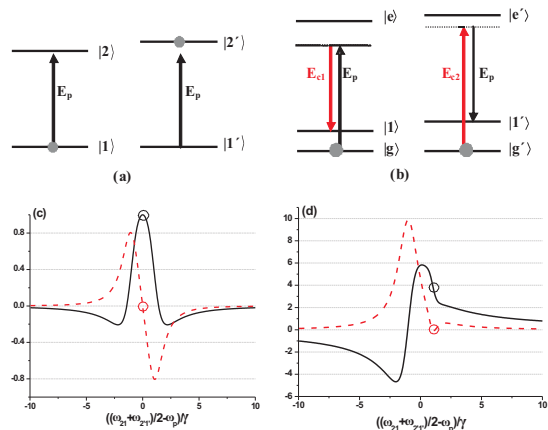


FIG. 1: (Color online) a) Two-component medium of two-level absorbing and amplifying systems; b) Two-component medium of three-level systems interacting with control and probe fields in a Raman configuration. The probe field experiences Raman absorption and amplification by the first and second system, respectively; c) Real (dashed line) $\Delta n'/(2\pi N|\mu_{21}|^2/\hbar)$ and imaginary (solid line) $\Delta n''/(2\pi N|\mu_{21}|^2/\hbar)$ parts of the complex refractive index for equal widths $\gamma = \gamma'$ of the absorbing and amplifying resonances, $N = N'$, $\Delta - \Delta' = 2\gamma$ and $\rho_{11} - \rho_{22} = -(\rho'_{11} - \rho'_{22}) = 1$. Frequencies of vanishing absorption accompanied by enhanced refractive index are shown by circles; d) Real (dashed line) and imaginary (solid line) parts of the complex refractive index for a wider absorbing resonance with $\gamma' = 0.5\gamma$, $N' = 0.1N$, $\Delta - \Delta' = 2\gamma$ and $\rho_{11} - \rho_{22} = -(\rho'_{11} - \rho'_{22}) = 1$.

When $\rho_{11} - \rho_{22} > 0$ and $\rho_{1'1'} - \rho_{2'2'} < 0$ the imaginary part of the refractive index $\Delta n''$ will be a superposition of absorbing and amplifying resonances, and $\Delta n'$ will show two frequency regions with normal and anomalous dispersion shifted with respect to each other. Depending on the frequency shift between the resonances it allows one to have enhanced or reduced refractive index with vanishing absorption shown by circles in Fig.1c. Vanishing absorption is accompanied in this case by amplification on the right side, and if the frequency fluctuates it will result in amplification of frequency fluctuations shifting the frequency to smaller index values. If the absorbing resonance is wider than the amplifying one and the energy difference between the two resonances is less than

the width of the wider resonance [14], it becomes possible to realize enhanced (or reduced) refractive index combined with zero absorption and no nearby gain. The corresponding real and imaginary parts of the refractive index are shown in Fig.1d.

We mentioned in the introduction that the difficulty of the two-level absorbing/amplifying scheme is the need for inversion for the amplifying two-level system. The frequencies of the absorbing and amplifying two-level systems are close and the pump, providing inversion, can degrade the population in the absorbing system. This problem can be avoided if three-level Raman systems are used, but in this case population has to be transferred into a specific ground state by optical pumping. As was observed in [16] optical pumping works efficiently only up to certain atomic density, which was $N \sim 1.2 \cdot 10^{14} \text{ cm}^{-3}$ in the case of ^{87}Rb . For higher densities, resulting in higher refractive index, optical pumping cannot populate a single ground state sublevel and degrades the system performance. In the next section we describe how the absorbing/amplifying system can be replaced by a single species four-level four-wave mixing system, which allows to have enhanced index with vanishing absorption without the need for inversion and optical pumping.

III. SUSCEPTIBILITY OF A FOUR-LEVEL FWM SYSTEM

We consider a four-level four-wave mixing scheme shown in Fig.2a. In the FWM medium there are two strong control fields at frequencies ω_{1c} and ω_{2c} , which we assume to have constant Rabi frequencies Ω_1 and Ω_2 , and two weak probe fields with different frequencies ω_1 and ω_2 :

$$E_j = \text{Re}(\mathcal{E}_j e^{-i\omega_j t + ik_j z}), \quad j = 1, 2, \quad (2)$$

where \mathcal{E}_1 and \mathcal{E}_2 are the field amplitudes. The density matrix equation for the system interacting with the fields is $\frac{d\hat{\rho}}{dt} = \frac{i}{\hbar} [\hat{\rho}, \hat{H}] + \mathcal{L}\hat{\rho}$, where $\hat{H} = \hat{H}_0 + \hat{H}_{int}$ and

$$\begin{aligned} \hat{H}_0 &= \hbar\omega_{41}|4\rangle\langle 4| + \hbar\omega_{31}|3\rangle\langle 3| + \hbar\omega_{21}|2\rangle\langle 2|, \\ \hat{H}_{int} &= -\tilde{\mu}_{41}\vec{E}|4\rangle\langle 1| - \tilde{\mu}_{32}\vec{E}|3\rangle\langle 2| - \tilde{\mu}_{31}\vec{E}|3\rangle\langle 1| \\ &\quad - \tilde{\mu}_{42}\vec{E}|4\rangle\langle 2| + H.c., \end{aligned} \quad (3)$$

$\vec{E} = \vec{E}_{c1} + \vec{E}_{c2} + \vec{E}_1 + \vec{E}_2$ and $\mathcal{L}\hat{\rho}$ is the Lindblad operator describing population and coherence decay. Elements of the density matrix obey the following equations:

$$\begin{aligned} \frac{d\sigma_{41}}{dt} &= -(i(\omega_{41} - \omega_1) + \gamma_{41})\sigma_{41} - i\alpha_1(\rho_{44} - \rho_{11}) \\ &\quad - i\Omega_1\sigma_{43} + i\Omega_2\sigma_{21}, \\ \frac{d\sigma_{32}}{dt} &= -(i(\omega_{32} - \omega_2) + \gamma_{32})\sigma_{32} - i\alpha_2(\rho_{33} - \rho_{22}) + \\ &\quad + i\Omega_1\sigma_{21}^* e^{-i\Delta kz} - i\Omega_2\sigma_{43}^* e^{-i\Delta kz}, \\ \frac{d\sigma_{21}}{dt} &= -(i(\omega_{21} - \omega_1 + \omega_2) + \gamma_{21})\sigma_{21} - i\Omega_1\sigma_{32}^* e^{-i\Delta kz} \end{aligned}$$

$$\begin{aligned} &-i\alpha_1\sigma_{42}^* + i\alpha_2^*\sigma_{31} e^{-i\Delta kz} + i\Omega_2^*\sigma_{41}, \\ \frac{d\sigma_{43}}{dt} &= -(i(\omega_{43} - \omega_1 + \omega_{c1}) + \gamma_{43})\sigma_{43} - i\Omega_1^*\sigma_{41} \\ &\quad - i\alpha_2^*\sigma_{42} e^{-i\Delta kz} + i\alpha_1\sigma_{31}^* + i\Omega_2\sigma_{32}^* e^{-i\Delta kz}, \\ \frac{d\sigma_{31}}{dt} &= -(i(\omega_{31} - \omega_{c1}) + \gamma_{31})\sigma_{31} - i\Omega_1(\rho_{33} - \rho_{11}) \\ &\quad - i\alpha_1\sigma_{43}^* + i\alpha_2\sigma_{21} e^{i\Delta kz}, \\ \frac{d\sigma_{42}}{dt} &= -(i(\omega_{42} - \omega_{c2}) + \gamma_{42})\sigma_{42} - i\Omega_2(\rho_{44} - \rho_{22}) \\ &\quad - i\alpha_2\sigma_{43} e^{i\Delta kz} + i\alpha_1\sigma_{21}^*, \\ \frac{d\rho_{11}}{dt} &= -i\Omega_1\sigma_{31}^* + i\Omega_1^*\sigma_{31} + \Gamma_{31}\rho_{33} + \Gamma_{41}\rho_{44}, \\ \frac{d\rho_{22}}{dt} &= -i\Omega_2\sigma_{42}^* + i\Omega_2^*\sigma_{42} + \Gamma_{32}\rho_{33} + \Gamma_{42}\rho_{44}, \\ \frac{d\rho_{33}}{dt} &= i\Omega_1\sigma_{31}^* - i\Omega_1^*\sigma_{31} - (\Gamma_{31} + \Gamma_{32})\rho_{33}, \\ \rho_{44} &= 1 - \rho_{11} - \rho_{22} - \rho_{33}, \end{aligned} \quad (4)$$

where $\sigma_{41} = \rho_{41} e^{i\omega_1 t - ik_1 z}$, $\sigma_{32} = \rho_{32} e^{i\omega_2 t - ik_2 z}$, $\sigma_{31} = \rho_{31} e^{i\omega_{c1} t - ik_{c1} z}$, $\sigma_{42} = \rho_{42} e^{i\omega_{c2} t - ik_{c2} z}$, $\sigma_{21} = \rho_{21} e^{i(\omega_1 - \omega_{c2})t - i(k_1 - k_{c2})z}$, $\sigma_{43} = \rho_{43} e^{i(\omega_1 - \omega_{c1})t - i(k_1 - k_{c1})z}$, $\alpha_1 = \mu_{41}\mathcal{E}_1/2\hbar$, $\alpha_2 = \mu_{32}\mathcal{E}_2/2\hbar$ are Rabi frequencies of the probe and $\Omega_1 = \mu_{31}E_{c1}/2\hbar$, $\Omega_2 = \mu_{42}E_{c2}/2\hbar$ are Rabi frequencies of the control fields, and $\Delta k = (\vec{k}_1 - \vec{k}_{c1} + \vec{k}_2 - \vec{k}_{c2})_z$ is the wavevector mismatch of the four fields. We assume the fields to propagate in z direction. Coherence and population decay rates are denoted as γ_{ij} and Γ_{ij} , respectively.

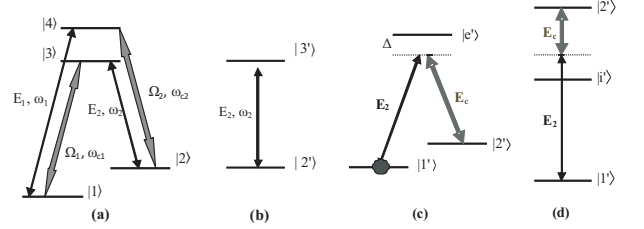


FIG. 2: a) Four-level four-wave mixing atomic system with two control fields (Rabi frequencies Ω_1 and Ω_2) close to resonance with the $|3\rangle - |1\rangle$ and $|4\rangle - |2\rangle$ transitions. The other transitions $|4\rangle - |1\rangle$ and $|3\rangle - |2\rangle$ interact with two probe fields E_1 and E_2 having frequencies ω_1 and ω_2 ; b) Absorbing two-level system providing vanishing probe absorption with no amplification on both sides; c), d) Additional absorption for one of the probe fields, e.g. for E_2 , can be realized via Raman or two-photon absorption using an additional control field E_c .

The medium polarization $P_j = \text{Re}(P_j e^{-i\omega_j t + ik_j z})$, $j = 1, 2$ at the frequencies ω_1 and ω_2 of the probe fields has an amplitude

$$\begin{aligned} P_1 &= N\mu_{14}\sigma_{41}, \\ P_2 &= N\mu_{23}\sigma_{32}, \end{aligned} \quad (5)$$

and is given by [17]:

$$\begin{aligned} P_1 &= \chi_{11}\mathcal{E}_1 + \chi_{12}e^{i\delta kz}\mathcal{E}_2^*, \\ P_2 &= \chi_{22}\mathcal{E}_2 + \chi_{21}e^{i\delta kz}\mathcal{E}_1^*, \end{aligned} \quad (6)$$

where χ_{ij} are the medium susceptibilities.

To simplify the analysis we assume that: 1) the control fields have equal Rabi frequencies $\Omega_1 = \Omega_2 = \Omega$ and are resonant with their corresponding transitions: $\omega_{42} - \omega_2 = 0$, $\omega_{31} - \omega_3 = 0$. Due to frequency matching condition $\omega_1 - \omega_{c1} = \omega_{c2} - \omega_2$ the probe fields then have detunings $\omega_{41} - \omega_1 = \delta$, $\omega_{32} - \omega_2 = -\delta$; 3) decay rates of excited states $|3\rangle$ and $|4\rangle$ are equal $\Gamma_3 = \Gamma_4 = \Gamma_r$ and $\Gamma_{ij} = \Gamma_r/2$, where $i = 3, 4$ and $j = 1, 2$, and Γ_r is the excited state radiative decay rate. Optical coherence decay rates are also assumed equal $\gamma_{ij} = \gamma$ for $i=3,4$ and $j=1,2$. Decay of the low-frequency coherence at the $|2\rangle - |1\rangle$ transition is assumed to be much slower than at optical transitions $\gamma_{21} \ll \gamma$. The corresponding susceptibilities are then given by [17]

$$\begin{aligned}\chi_{11} &= \frac{i|\mu_{41}|^2 N}{2\hbar} (\rho_{ll} - \rho_{uu}) \frac{i\delta + \gamma_{21} - i\delta\Omega^2/(\gamma(\gamma + i\delta))}{(i\delta + \gamma)(i\delta + \gamma_{21}) + 2|\Omega|^2}, \\ \chi_{12} &= -i \frac{\mu_{41}\mu_{32}^* N}{2\hbar\gamma(i\delta + \gamma)} \frac{\Omega^2(\rho_{ll} - \rho_{uu})(i\delta + 2\gamma)}{(i\delta + \gamma)(i\delta + \gamma_{21}) + 2|\Omega|^2}, \\ \chi_{22} &= \frac{i|\mu_{32}|^2 N}{2\hbar} (\rho_{ll} - \rho_{uu}) \frac{-i\delta + \gamma_{21} + i\delta\Omega^2/(\gamma(\gamma - i\delta))}{(-i\delta + \gamma)(-i\delta + \gamma_{21}) + 2|\Omega|^2}, \\ \chi_{21} &= -i \frac{\mu_{41}^*\mu_{32} N}{2\hbar\gamma(-i\delta + \gamma)} \frac{\Omega^2(\rho_{ll} - \rho_{uu})(-i\delta + 2\gamma)}{(-i\delta + \gamma)(-i\delta + \gamma_{21}) + 2|\Omega|^2},\end{aligned}\quad (7)$$

where the population difference between the ground and excited states, assuming for simplicity equal dipole moments of optical transitions $\mu_{41} = \mu_{42} = \mu_{32} = \mu_{31} = \mu$ is given by

$$\rho_{ll} - \rho_{uu} = \frac{1}{2} \frac{1}{1 + 4\Omega^2/\gamma\Gamma_r}. \quad (8)$$

As a result, propagation equations for the two probe fields look as follows:

$$\begin{aligned}\frac{\partial \mathcal{E}_1}{\partial z} &= 2\pi i k_1 \chi_{11} \mathcal{E}_1 + 2\pi i k_1 \chi_{12} e^{i\Delta k z} \mathcal{E}_2^*, \\ \frac{\partial \mathcal{E}_2}{\partial z} &= 2\pi i k_2 \chi_{22} \mathcal{E}_2 + 2\pi i k_2 \chi_{21} e^{i\Delta k z} \mathcal{E}_1^*.\end{aligned}\quad (9)$$

Setting for simplicity $\Delta k = 0$ we can find from Eqs.(9) propagation constants for the probe fields:

$$\begin{aligned}\lambda^\pm &= i\pi(k_1\chi_{11} - k_2\chi_{22}^*) \pm \\ &\pm i\pi\sqrt{(k_1\chi_{11} + k_2\chi_{22}^*)^2 - 4k_1k_2\chi_{12}\chi_{21}^*}.\end{aligned}\quad (10)$$

Assuming $k_1 \approx k_2 = k$ (e.g. states $|1\rangle$ and $|2\rangle$ and similarly $|3\rangle$ and $|4\rangle$ are hyperfine sublevels of the same electronic level) and using $\chi_{22} = -\chi_{11}^*$ and $\chi_{21} = -\chi_{12}^*$ we have

$$\lambda^\pm = 2\pi i k (\chi_{11} \pm \chi_{12}). \quad (11)$$

The change in the refractive index $\Delta n = \Delta n' + i\Delta n''$ induced by the FWM medium can be found from the propagation constants as $\Delta n'_\pm = \text{Im}\lambda_\pm/k$ and $\Delta n''_\pm = -\text{Re}\lambda_\pm/k$. Typical shapes of the imaginary and real

parts of the refractive index $\Delta n''$ and $\Delta n'$ in this idealized four-level medium are shown in Figs.3a and 3b. The index is calculated for a range of atomic densities N described by a dimensionless parameter $r = \pi|\mu|^2 N/\hbar\Gamma_r$. Taking into account that $\Gamma_r = 4k^3|\mu|^2/3\hbar$ gives $r = 3N\lambda^3/64\pi^2$, where $\lambda = 2\pi/k$, which determines the maximal possible index enhancement. One can see that for λ_+ there are regions of enhanced and reduced index accompanied by zero absorption (and amplification). The frequency corresponding to vanishing absorption, which at the same time corresponds to maximal refractive index, is denoted by a vertical dotted line. The λ_- constant is always accompanied by non-zero absorption, as shown in Fig.3c. The enhanced refractive index in the FWM system is realized without inversion or optical pumping, populations are assumed to be redistributed by the control fields.

We can estimate the maximal possible index enhancement in the idealized FWM system. From Eq.(11) the complex index $\Delta n_+ = \lambda_+/ik$ equals

$$\Delta n_+ = \frac{i\pi N|\mu|^2}{\hbar} (\rho_{ll} - \rho_{uu}) \frac{i\delta + \gamma_{21} - 2\Omega^2/\gamma}{(i\delta + \gamma)(i\delta + \gamma_{21}) + 2\Omega^2}. \quad (12)$$

Absorption vanishes when the imaginary part of the index $\Delta n''_+ = 0$ at $\delta^2 = \frac{4\Omega^4/\gamma^2 - \gamma_{21}^2}{1 + 2\Omega^2/\gamma^2}$. The corresponding real part of the index at this frequency is given by $\Delta n'_+ = rF$, where

$$\begin{aligned}F &= \frac{\Gamma_r/\gamma}{(1 + 4\Omega^2/\gamma\Gamma_r)} \sqrt{\frac{4\Omega^4/\gamma^4 - \gamma_{21}^2/\gamma^2}{1 + 2\Omega^2/\gamma^2}} \times \\ &\times \frac{(2(1 + \Omega^2/\gamma^2) - \gamma_{21}/\gamma)(1 + 2\Omega^2/\gamma^2)}{(1 + \gamma_{21}/\gamma)(4\Omega^2(1 + \Omega^2/\gamma^2)/\gamma^2 + \gamma_{21}(2 - \gamma_{21}/\gamma)/\gamma)}.\end{aligned}\quad (13)$$

The factor F is maximized for some Rabi frequency of the control fields, the corresponding dependence is shown in Fig.4 for a range of low-frequency coherence decay rates γ_{21} . It shows that for small enough $\gamma_{21} \leq 10^{-3}\gamma$ the maximal value of $F \sim \Gamma_r/\gamma$. It allows us to estimate the maximal possible enhancement of the refractive index in the four-level FWM medium: $\Delta n'_{+,max} = r\Gamma_r/\gamma \approx 3N\Gamma_r\lambda^3/64\gamma\pi^2$. Using as an example a D1 transition of ^{40}K with $\lambda = 770.1$ nm we get $\Delta n'_{+,max} = 2.17 \cdot 10^{-15}\Gamma_r N(\text{cm}^{-3})/\gamma$. We obtain therefore that for radiatively broadened optical transitions with $\gamma = \Gamma_r/2$ (where $\Gamma_r = 6.035$ MHz for the D1 line) $\Delta n'_+ \approx 0.43$ already for $N = 10^{14} \text{ cm}^{-3}$ and even larger index change can be realized for higher densities.

IV. INDEX ENHANCEMENT IN THE PRESENCE OF COLLISIONAL AND DOPPLER BROADENING

Large enhancement of refractive index ($\Delta n' \sim 4$ in Fig.3a) obtained in the previous section assumes radiatively broadened optical transitions. For large atomic densities, however, collisional broadening has to be taken

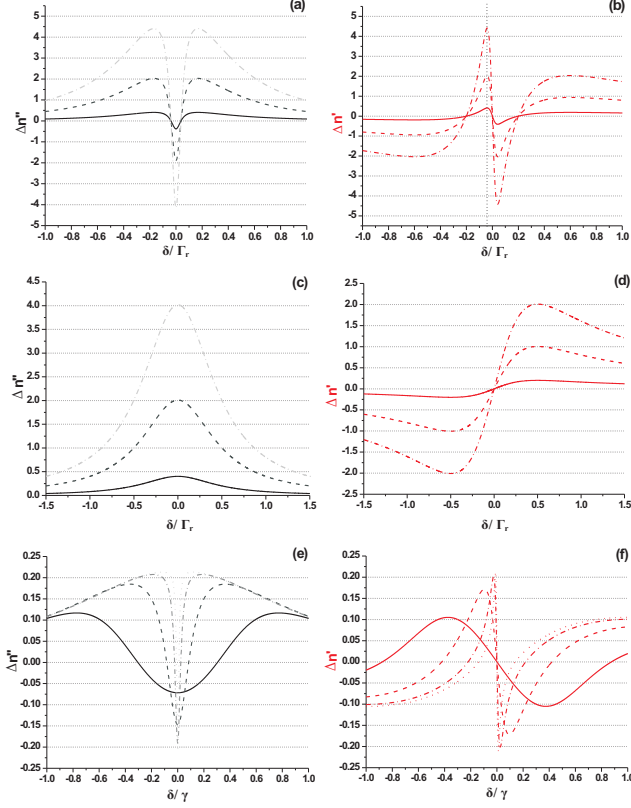


FIG. 3: (Color online) a) Imaginary (grey lines) and b) real (red lines) parts of the refractive index change Δn , corresponding to the λ_+ propagation constant. Curves are shown for a range of atomic densities given by the parameter $r = \pi|\mu|^2 N/2\hbar\Gamma_r = 3N\lambda^3/64\pi^2$. Solid, dashed and dash-dotted lines correspond to $N = 10^{14}$, $5 \cdot 10^{14}$ and 10^{15} cm^{-3} . Other parameters are: $\lambda = 770.1 \text{ nm}$, $\gamma = \Gamma_r/2$, $\gamma_{21} = 10^{-3}\Gamma_r$ and $\Omega = 0.1\Gamma_r$. The vertical dotted line denotes the frequency of maximal refractive index with vanishing absorption; c) Imaginary and d) real parts of the refractive index corresponding to λ_- for the same densities; e),f) Dependence of index enhancement on the low-frequency coherence decay rate γ_{21} : e) imaginary (grey lines) and f) real (red lines) parts of the index change corresponding to λ_+ for a range of decay rates γ_{21} . Solid, dashed, dash-dotted and dotted lines correspond to $\gamma_{21} = 0.1\gamma$, 0.01γ , 0.001γ and 0.0001γ ; $N = 10^{14} \text{ cm}^{-3}$ and Ω maximizing $\Delta n'$ according to Eq.(13) was used.

into account adding a contribution γ_{coll} to the optical coherence decay rate $\gamma = \Gamma_r/2 + \gamma_{coll}$. In order to get a more realistic estimate of index enhancement we will analyze the D1 transition of ^{40}K taking into account its multi-level structure. The ground $4 S_{1/2}$ and excited $4 P_{1/2}$ states of ^{40}K are each split in two hyperfine sublevels with $F = 9/2, 7/2$ ($F = 9/2$ state being lower in energy) due to the nuclear spin $I = 4$ of ^{40}K . The hyperfine splittings are 1.286 GHz in the ground and 0.155 GHz in the excited state [18], as shown in Fig.5a. Four levels of the FWM scheme can be associated with the hyperfine states

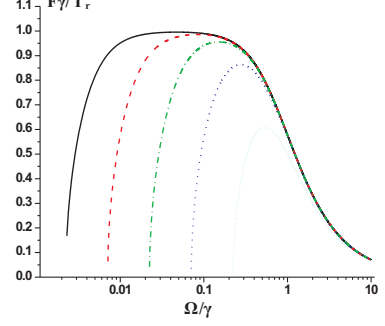


FIG. 4: (Color online) Dependence of the F coefficient given by Eq.(13) on the Rabi frequency of the control fields for a range of low-frequency coherence decay rates γ_{21} . Increasing F corresponds to $\gamma_{21} = 10^{-1}\gamma$ (light blue short-dotted curve), $10^{-2}\gamma$ (blue dotted curve), $10^{-3}\gamma$ (green dash-dotted curve), $10^{-4}\gamma$ (red dashed curve) and $10^{-5}\gamma$ (black solid curve), where $\gamma = \Gamma_r/2$.

as $|1\rangle = |4 S_{1/2}, F = 9/2\rangle$, $|2\rangle = |4 S_{1/2}, F = 7/2\rangle$ and $|3\rangle = |4 P_{1/2}, F' = 9/2\rangle$, $|4\rangle = |4 P_{1/2}, F' = 7/2\rangle$. We assume that the control and probe fields are π polarized, coupling all $|F, m_F\rangle$ ground state to all $|F', m_F\rangle$ excited state hyperfine sublevels, respectively.

The fractional hyperfine quantum numbers of ^{40}K make all transitions $|F, m_F\rangle \leftrightarrow |F', m_F\rangle$ allowed, which does not happen for integer hyperfine numbers in the case of e.g. Rb and Cs. In the latter case the $|F, m_F = 0\rangle \leftrightarrow |F' = F, m'_F = 0\rangle$ transition is forbidden, resulting in optical pumping of all population into the dark $|F, m_F = 0\rangle$ state and vanishing light-matter interaction. One can try to use circularly polarized fields to overcome this difficulty, but in this case all population will be optically pumped into another dark state $|F, m_F = F\rangle$ and light-matter interaction vanishes again. Therefore, to counteract optical pumping into dark states in systems with integer hyperfine numbers some sort of repumping has to be used. Fractional hyperfine quantum numbers of ^{40}K allow one to avoid pumping population into dark states, and as a result no repumping is needed.

We can now estimate the index enhancement in the four-level system of the previous section at large atomic densities taking into account collisional broadening of optical transitions. The broadening rate for the D1 transition of K is $2\gamma_{coll} = 2\beta N = 0.7 \cdot 10^{-13} N (\text{cm}^{-3})$ MHz according to [19]. Maximal possible refractive index enhancement is then given by $\Delta n'_{+max} = 2.17 \cdot 10^{-15} \Gamma_r N / (\Gamma_r/2 + \beta N)$, resulting in theoretical maximal value $\Delta n'_{+max} \approx 2.17 \cdot 10^{-15} \Gamma_r / \beta \approx 0.37$ for $N \gg \Gamma_r/2\beta = 8.6 \cdot 10^{13} \text{ cm}^{-3}$.

In order to get a better estimate for index enhancement we considered interaction of the π polarized control and probe fields with the real multilevel structure of the ^{40}K D1 line, taking into account transition dipole moments and population decay rates from [18]. The index

change in the presence of collisional broadening is shown in Figs.5b and 5c. One can see that in the real system the maximal index change is reduced with respect to the theoretical estimate to $\Delta n'_+ \approx 0.1$, but is still high.

So far we have considered the situation which corresponds to cold gases with vanishing Doppler broadening. In warm and hot atomic vapors Doppler broadening has to be taken into account. We included its effect by numerically averaging propagation constants (10) over the 1D Maxwell-Boltzmann distribution $f(\delta\omega) = \exp(-(\delta\omega/W_D)^2)/\sqrt{\pi}W_D$, where $\delta\omega = kv_z$ is the Doppler frequency shift of an atom having velocity v_z along the propagation axis z ; $W_D = k\sqrt{2k_B T/m}$ is the width of the Doppler profile. Due to a small mass of ^{40}K the Doppler width is large even at room temperature ($W_D = 458$ MHz at $T = 300$ K), exceeding the hyperfine splitting in the $4 P_{1/2}$ state. It will result in interaction of all fields with both $|3\rangle = |F' = 9/2\rangle$ and $|4\rangle = |F' = 7/2\rangle$ states, complicating the analysis. To avoid this complication we assumed that the state $|4\rangle = |F' = 9/2\rangle$ belongs to the $4 P_{3/2}$ excited state, i.e. to the D2 line. We again took into account dipole moments and population decay rates for transitions between $|F, m_F\rangle$ and $|F' = 9/2, m_F\rangle$ of the D2 line from [18].

The temperature not only controls the Doppler width but vapor density as well, making it temperature dependent. The pressure-temperature and density-pressure dependence for K vapor is the following [18]

$$\begin{aligned} \log_{10} p &= 7.9667 - \frac{4646}{T}, & 298 \text{ K} < T < 336.8 \text{ K}, \\ \log_{10} p &= 7.4077 - \frac{4453}{T}, & 336.8 \text{ K} < T < 600 \text{ K}, \\ N &= \frac{10^2 p}{k_B T}, & (14) \end{aligned}$$

where p is in mbar, T in K and N is in m^{-3} . The resulting complex index Δn_+ corresponding to the λ_+ propagation constant is given in Figs.5b and 5c for several temperatures. One can see that for high temperatures $T \sim 600$ K the index change is $\Delta n'_+ \approx 0.01$, i.e. about an order of magnitude smaller than in a cold gas without Doppler broadening.

Finally, we discuss briefly how the probe fields propagate in a medium of finite thickness. From Fig.3 we know that the imaginary part of Δn_- is positive, i.e. corresponds to absorption for all detunings. As a result, the λ_- component will be attenuated during propagation, while the λ_+ component will get amplified or stay constant at the frequency of vanishing absorption. Eqs.(9) can be solved to obtain the following finite thickness solutions for the fields:

$$\begin{aligned} E_1(z=L) &= e^{i\pi\delta a L} [E_1(z=0) (i(k_1\chi_{11} + k_2\chi_{22}^*) \sin(\pi SL) + \\ &\quad + S \cos(\pi SL)) / S + E_2^*(z=0) 2ik_1\chi_{12} \sin(\pi SL) / S], \\ E_2^*(z=L) &= e^{i\pi\delta a L} [-2ik_2\chi_{21}^* \sin(\pi SL) E_1(z=0) / S + \\ &\quad + E_2^*(z=0) (\cos(\pi SL) - i(k_1\chi_{11} + k_2\chi_{22}^*) \sin(\pi SL) / S)], \end{aligned} \quad (15)$$

where $\delta a = \frac{k_1\chi_{11} - k_2\chi_{22}^*}{\sqrt{(k_1\chi_{11} + k_2\chi_{22}^*)^2 - 4k_1k_2\chi_{12}\chi_{21}^*}}$, $S = L$ is the medium thickness, $E_{1,2}(z=0)$ are the field amplitudes at the medium entrance. At a distance $|Im\lambda_-|L \gg 1$ Eqs.(15) have the form:

$$\begin{aligned} E_1(z=L) &\sim \frac{1}{2S} e^{i\lambda_+ L} (E_1(z=0)(k_1\chi_{11} + k_2\chi_{22}^* + S) + \\ &\quad + 2k_1\chi_{12} E_2^*(z=0)), \\ E_2^*(z=L) &\sim \frac{1}{2S} e^{i\lambda_+ L} (-2k_2\chi_{21}^* E_1(z=0) + \\ &\quad + E_2^*(z=0)(S - k_1\chi_{11} - k_2\chi_{22}^*)), \end{aligned}$$

which shows that it suffices to have a single field at the medium entrance, e.g. the $E_1(z=0)$ field, to realize index enhancement. The second field will be generated during propagation due to four-wave mixing process.

We also note that the four-wave mixing system can have another interesting application. It can be used to realize parity-time (PT) symmetric complex index of refraction obeying the condition $n(x,t) = n^*(-x,-t)$, i.e. with real and imaginary parts of the index being even and odd functions in time and space, respectively. The PT symmetric refractive index allows to model non-Hermitian Hamiltonians of the Schrodinger equation having real eigenvalues, related to discussions on fundamentals of quantum mechanics based on axioms of Hermitian operators for observables. The complex index derived from propagation constants (10) has the required symmetry with respect to frequency inversion $\omega \rightarrow -\omega$, which is equivalent to time inversion $t \rightarrow -t$. The symmetries of n' and n'' with respect to inversion in space can be realized using far-detuned control fields propagating in x direction producing spatially dependent Stark shifts [20].

V. COMPOSITE FWM AND TWO-LEVEL ABSORBING SYSTEM

In the previous section we showed that enhanced refractive index accompanied by vanishing absorption can be realized in a four-level atomic system in the regime of four-wave mixing. However, one can see from Figs.3 and 5 that there is amplification on the right side of the vanishing absorption point, which will amplify frequency components of the probe pulse in this region. Vanishing absorption with no nearby amplification is possible if an additional absorbing atomic component is added to the system. Absorption for one of the probe fields, e.g. for the E_2 field, can be realized by a two-level system shown in Fig.2b. In this case the total susceptibility at the ω_2 frequency is $\chi_{22} = \chi_{22}^{FWM} + \chi_{22}^{abs}$, where χ_{22}^{FWM} is given by Eq.(7) and the contribution to susceptibility from the two-level system is

$$\chi_{22}^{abs} = i \frac{|\mu'_{32}|^2 N'}{\hbar} \frac{1}{i(\omega'_{32} - \omega_2) + \gamma'_{32}}, \quad (16)$$

where the detuning $\omega'_{32} - \omega_2 = -\delta + \delta_0$, $\delta_0 = \omega'_{32} - \omega_{32}$ is the frequency difference of the transitions in the two and four-level systems, and $\delta = -(\omega_{32} - \omega_2)$ is the detuning for the four-level system.

The propagation constants for the composite system can be calculated from Eq.(10) using the modified χ_{22} . Fig.6a shows the corresponding real and imaginary parts of the complex index corresponding to λ_{\pm} assuming the idealized radiatively broadened four-level system described by Eqs.(7) and a radiatively broadened two-level system. One can see that for the λ_+ constant there is vanishing absorption at $\delta/\Gamma_r \approx -0.42$ accompanied by enhanced refractive index, shown by the vertical line, with no amplification on either sides. The index change corresponding to λ_- , shown in the inset to Fig.6a, displays strong absorption at the frequency of vanishing absorption of λ_+ .

The absorbing system can also be realized by a Raman or two-photon transition shown in Fig.2c. The advantage of the Raman and two-photon configurations is that the optical transition frequency does not have to be near resonant with the probe field. In this case resonant absorption for the probe field will be provided by the two-photon resonance of the probe and a control field E_c with the transition $|2'\rangle - |1'\rangle$. An additional and important advantage of the Raman scheme is that the resonance can be quite narrow, much narrower than the optical one, which we found necessary to have vanishing absorption with no nearby amplification in Fig.6.

To have a more realistic estimate of the index enhancement in the composite case we considered a two-species medium of ^{40}K and ^{39}K atomic gases. The ^{40}K isotope provides the four-level system analyzed in the previous section, and ^{39}K allows to realize absorption for one of the probe fields, specifically, for the E_2 field. The two isotopes of which ^{39}K is more abundant (93.26%) than ^{40}K (0.01%) have the same D1 transition wavelength $\lambda = 770.1$ nm, but different hyperfine structure, due to the ^{39}K nuclear spin of 3/2. The corresponding level scheme is shown in Fig.6b. One can see that resonant absorption for E_2 can be realized in a Raman scheme where the probe and an additional control field are near two-photon resonant with the $F = 1 \leftrightarrow F = 2$ hyperfine transition of $4 S_{1/2}$ state of ^{39}K . In numerical calculations we assumed that the control field has the same π polarization as the probe one and took into account fields interaction with all $|F, m_F\rangle \leftrightarrow |F', m_F\rangle$ transitions, where $F = 1, 2$ and $F' = 1, 2$ are the hyperfine sublevels of the $4 S_{1/2}$ and $4 P_{1/2}$ states of ^{39}K . We also took into account collisional broadening of the op-

tical transitions of both isotopes using the total atomic density $N = N_{40K} + N_{39K}$. The complex index change corresponding to the λ_+ propagation constant is shown in Fig.6c. The refractive index at the vanishing absorption point is enhanced by $\Delta n'_+ \sim 10^{-2}$ in the case of $N_{40K} = 10^{14}$ cm^{-3} and $N_{39K} = 10N_{40K}$, shown by the vertical line.

VI. CONCLUSIONS

We analyzed a possibility to realize enhanced refractive index with vanishing absorption in a four-level four-wave mixing atomic system. The susceptibility of the FWM system displays frequency regions where absorption turns into amplification accompanied by non-zero refractive index, leading to enhanced refractive index with zero absorption in this medium. Index enhancement in the FWM system is more robust compared to previously considered approaches using a three-level coherence-based Λ scheme and a composite absorbing/amplifying scheme because it allows one to avoid pumping population into dark states and does not require inversion or pumping population into specific states. Although optical pumping of population into dark states does not take place in ideal three or two-level schemes, it becomes an issue in real multilevel atomic systems, e.g. in alkali gases. We analyzed a particular system of ^{40}K gas, which does not have this problem, and found that refractive index enhancement $\Delta n \sim 0.1$ is possible in a cold gas with vanishing Doppler broadening at densities $N \sim 10^{15}$ cm^{-3} . The index change is $\Delta n \sim 10^{-2}$ if both collisional and Doppler broadening are present. We note that these predictions give larger index change compared to observed experimentally so far by two orders of magnitude.

We showed also that enhanced refractive index accompanied by vanishing absorption with no nearby amplification can be realized in a composite system including four-level four-wave mixing and two-level absorbing species. As an example we considered a combination of ^{40}K and ^{39}K atomic gases, where the first system provides FWM and the second one provides additional absorption for one of the probe fields. Analysis of the complex index of the composite system taking into account interaction of the fields with multilevel atomic structures and collisional broadening showed that index enhancement $\Delta n \sim 10^{-2}$ can be realized at a frequency of vanishing absorption with no nearby amplification.

The authors gratefully acknowledge financial support from the Russian Quantum Center and NSF.

-
- [1] *Principles of Optics*, by M. Born and E. Wolf, Cambridge University Press, Cambridge, UK (1999).
 [2] M. Fleischhauer, A. Imamoglu, J. P. Marangos, Rev. Mod. Phys. **77**, 633 (2005).
 [3] A. Kasapi, M. Jain, G.Y. Yin, S.E. Harris, Phys. Rev.

- Lett. **74**, 2447 (1995); L. V. Hau, S. E. Harris, Z. Dutton, C. H. Behroozi, Nature **397**, 594 (1999); M.M. Kash, V.A. Sautenkov, A.S. Zibrov, L. Hollberg, G.R. Welch, M.D. Lukin, Y. Rostovtsev, E.S. Fry, M.O. Scully, Phys. Rev. Lett. **82**, 5229 (1999).

- [4] M. Fleischhauer, M.D. Lukin, Phys. Rev. Lett. **84**, 5094 (2000); D.F. Phillips, A. Fleischhauer, A. Mair, R.L. Walsworth, M.D. Lukin, Phys. Rev. Lett. **86**, 783 (2001); C. Liu, Z. Dutton, C.H. Behroozi, L.V. Hau, Nature **409**, 6819 (2001).
- [5] V. G. Veselago, Sov. Phys. Usp. **10**, 509 (1968).
- [6] J. B. Pendry, Phys. Rev. Lett. **85**, 3966 (2000).
- [7] L. Novotny, B. Hecht, *Principles of Nano-Optics*, Cambridge University Press, Cambridge, UK, 2006.
- [8] J.B. Pendry, D. Schurig, D.R. Smith, Science **312**, 1780 (2006); U. Leonhardt, Science **312**, 1777 (2006); T. Ergin, N. Stenger, P. Brenner, J.B. Pendry, M. Wegener, Science **328**, 337 (2010); X. Chen, Y. Luo, J. Zhang, K. Jiang, J.B. Pendry, S. Zhang, Nat. Commun. **2**, 176 (2010).
- [9] J.B. Pendry, Science **306**, 1353 (2004).
- [10] J. Kastel, M. Fleischhauer, S. F. Yelin, R. L. Walsworth, Phys. Rev. Lett. **99**, 073602 (2007).
- [11] M.O. Scully, Phys. Rev. Lett. **67**, 1855 (1991); M. Fleischhauer, C.H. Keitel, M.O. Scully, C. Su, B.T. Ulrich, S.Y. Zhu, Phys. Rev. A **46**, 1468 (1992); U. Rathe, M. Fleischhauer, S.Y. Zhu, T.W. Hansch, M.O. Scully, Phys. Rev. A **47**, 4994 (1993).
- [12] A. S. Zibrov, M. D. Lukin, L. Hollberg, D. E. Nikonov, M. O. Scully, H. G. Robinson, V. L. Velichansky, Phys. Rev. Lett. **76**, 3935 (1996).
- [13] D.D. Yavuz, Phys. Rev. Lett. **95**, 223601 (2005).
- [14] C. O'Brien, P.M. Anisimov, Y. Rostovtsev, O. Kocharovskaya, Phys. Rev. A **84**, 063835 (2011).
- [15] N. A. Proite, B. E. Unks, J. T. Green, D. D. Yavuz, Phys. Rev. Lett. **101**, 147401 (2008).
- [16] Z. J. Simmons, N. A. Proite, J. Miles, D. E. Sikes, D. D. Yavuz, Phys. Rev. A **85**, 053810 (2012).
- [17] M. D. Lukin, P.R. Hemmer, M. Lffler, M. O. Scully, Phys. Rev. Lett. **81**, 2675 (1998).
- [18] <http://staff.science.uva.nl/walraven/Publications-files/PotassiumProperties.pdf>
- [19] H. van Kampen, A. V. Papoyan, V. A. Sautenkov, P. H. A. M. Castermans, E. R. Eliel, J. P. Woerdman, Phys. Rev. A **56**, 310 (1997).
- [20] C. Hang, G. Huang, V. V. Konotop, Phys. Rev. Lett. **110**, 083604 (2013).

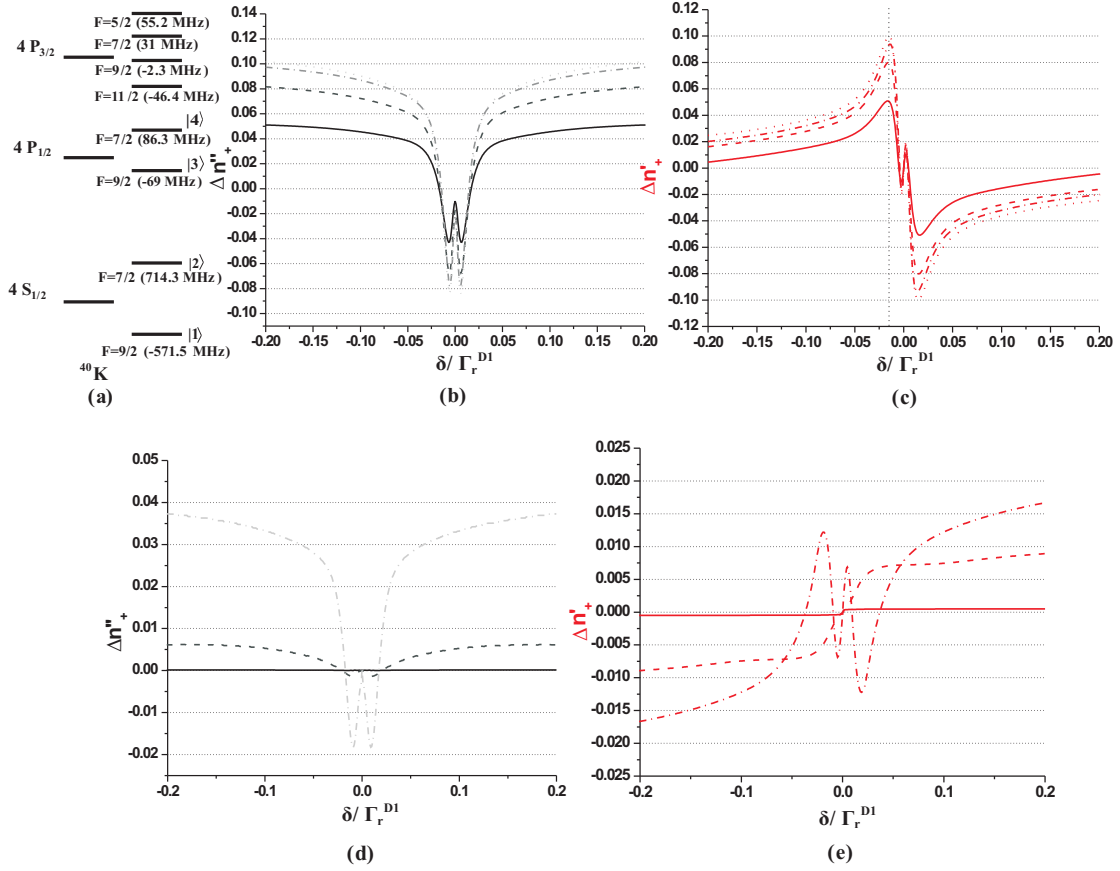


FIG. 5: (Color online) a) Hyperfine structure of the $4S_{1/2}$, $4P_{1/2}$ and $4P_{3/2}$ states of ^{40}K , including level shifts relative to centers of D1 and D2 transitions. Hyperfine states forming the FWM scheme are also shown; b) Imaginary (grey lines) and c) real (red lines) parts of the complex index change for a four-level scheme formed by hyperfine transitions of ^{40}K D1 line, taking into account collisional broadening. Solid, dashed, dash-dotted and dotted lines correspond to the density of K vapor is $N = 10^{14}$, $5 \cdot 10^{14}$, 10^{15} and $5 \cdot 10^{15}$ cm^{-3} . The frequency corresponding to vanishing absorption and enhanced index is shown by a vertical dotted line; d) Imaginary (grey lines) and e) real (red lines) parts of the complex index change for a four-level scheme formed by hyperfine transitions of the ^{40}K D1 and D2 lines (see text) taking into account collisional and Doppler broadenings. Solid, dashed, and dash-dotted lines correspond to the temperature of K vapor $T = 300$, 450 and 600 K.

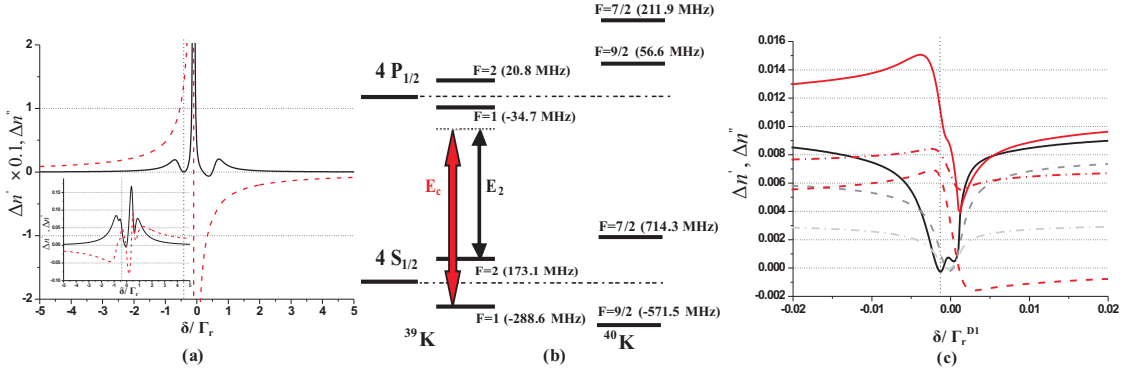


FIG. 6: (Color online) a) Real (red dashed line) and imaginary (black solid line) parts of the complex index change for the λ_+ constant of the composite four and two-level system. Ideal four-level FWM plus a two-level absorbing systems are assumed with the susceptibilities given by Eqs.(7), (16). The frequency corresponding to vanishing absorption with no nearby amplification is shown by a vertical dotted line. Parameters are: $N_{FWM} = 10^{14} \text{ cm}^{-3}$, $N_{abs} = 10N_{FWM}$, $\gamma = \Gamma_r/2$, $\gamma_{abs} = 10^{-3}\Gamma_r/2$, $\delta_0 = 0.1\Gamma_r$, $\Omega = 0.45\Gamma_r$, where Γ_r is the radiative decay rate of excited states in the four-level system; b) Hyperfine structure of D1 transitions of ^{39}K and ^{40}K including level shifts relative to transition center. Shown also the Raman transition for E_2 and an additional control field near resonant with $F = 1 \leftrightarrow F = 2$ of ^{39}K providing absorption for the probe field; c) Real (red lines) and imaginary (grey lines) parts of the complex index change for λ_+ propagation constant in the $^{39}\text{K}+^{40}\text{K}$ system. Solid lines correspond to $N_{40K} = 10^{14} \text{ cm}^{-3}$, $N_{39K} = 10N_{40K}$, $\Omega_{c1} = \Omega_{c2} = 1.3\Gamma_r^{D1}$, $\Omega_c = 10\Gamma_r^{D1}$, $\delta_0 = -0.92\Gamma_r^{D1}$, $\gamma_{9/2,7/2} = \gamma_{21} = 10^{-3}\Gamma_r^{D1}$; dashed lines correspond to $N_{40K} = 5 \cdot 10^{14} \text{ cm}^{-3}$, $N_{39K} = 15N_{40K}$, $\Omega_{c1} = \Omega_{c2} = 2.3\Gamma_r^{D1}$, $\Omega_c = 20\Gamma_r^{D1}$, $\delta_0 = -3\Gamma_r^{D1}$, $\gamma_{9/2,7/2} = \gamma_{21} = 10^{-3}\Gamma_r^{D1}$; short-dashed lines correspond to $N_{40K} = 10^{15} \text{ cm}^{-3}$, $N_{39K} = 25N_{40K}$, $\Omega_{c1} = \Omega_{c2} = 4.4\Gamma_r^{D1}$, $\Omega_c = 20\Gamma_r^{D1}$, $\delta_0 = -3\Gamma_r^{D1}$, $\gamma_{9/2,7/2} = \gamma_{21} = 10^{-3}\Gamma_r^{D1}$, where Γ_r^{D1} is the radiative decay rate of the D1 transition of ^{40}K .